Steel and Composite Structures, *Vol. 19, No. 3 (2015) 759-776*
DOI: http://dx.doi.org/10.12989/scs.2015.19.3.759

Dynamic behavior of piezoelectric bimorph beams with a delamination zone

Adel Zemirline [*1,2], Mohammed Ouali [1a] and Ali Mahieddine [3b]

[1] *Laboratory of Research*: "*Structures*" *In the University of Saad Dahleb*, *Blida 09000*, *Algeria*
[2] *The LMP2M laboratory*, *In the University of Yahia Fares*, *Ain D'heb Medea 26000, Algeria*
[3] *Energy and smart systems Laboratory*, *Khemis Miliana University*, *Algeria*

(*Received December 16, 2014, Revised March 19, 2015, Accepted April 02, 2015*)

Abstract. The First Order Shear Deformation Theory (FOSDT) is considered to study the dynamic behavior of a bimorph beam. A delamination zone between the upper and the lower layer has been taken into consideration; the beam is discretised using the finite elements method (FEM). Several parameters are taken into consideration like structural damping, the geometry, the load nature and the configurations of the boundary conditions. Results show that the delamination between the upper and the lower layer affects considerably the actuation.

Keywords: piezoelectricity; bimorph beam; delamination; shear deformation

1. Introduction

The actuation domain knows a great progress with the introduction of the piezoelectric materials; they allowed obtaining lightweight and precise actuators. More researches are devoted last years to the application of this actuators in several domains, essentially aeronautics, aerospace, automobile and more. The modeling of the structures made of beams knows a great diversity between the authors.

Lui *et al*. (2012) presented a method to estimate the energy conversion efficiency of the rainbow shape piezoelectric transducer. The research results show that both the shape parameters and elastic modulus exert great influence on energy conversion efficiency and the results obtained from analytical equation are in a good agreement with those from FE results and experimental results. Zhou *et al*. (2007) have established an analytical sandwich beam model for piezoelectric bender elements, based on first-order shear deformation theory (FSDT), which assumes reasonable distribution functions for electric potential in piezoelectric layers, and introduces proper shear correction factor k to account for the nonlinear transverse shear strain. The accuracy of the presented model especially for lower vibration modes was proved by free vibration analysis of

*Corresponding author, Ph.D. Student, E-mail: zemirline.adel@yahoo.com
[a] Professor, E-mail: oualimohammed@yahoo.fr
[b] Ph.D., E-mail: mahieddine.ali@gmail.com

http://www.techno-press.org/?journal=scs&subpage=8 ISSN: 1229-9367 (Print), 1598-6233 (Online)

simply-supported bender elements which presents an efficient analytical model for dynamic response analysis of piezoelectric bender elements. Donoso and Sigmund (2009) were interested in controlling the tip-deflection of a cantilever beam subjected to static and time-harmonic loading on its free end; the beam has a variable thickness and a variable width. Firstly, the profile of the thickness of a piezoelectric bimorph actuator is optimized, and secondly the profile of the width. They concluded that the different thickness values can take the same bending moment value indicating non-uniqueness of the results. Li *et al*. (2014) developed a model with a size-dependent functionally graded piezoelectric beam using a variational formulation. It is based on the modified strain gradient theory and Timoshenko beam theory. The material properties of functionally graded piezoelectric beam are assumed to vary through the thickness according to a power law. Nikkho (2014) studied an Euler–Bernoulli beam, with a number of piezoelectric patches bonded on the bottom and top surfaces, the constitutive equation of motion which is derived by employing Hamilton's principle are developed for the beam subjected to arbitrary boundary conditions. A classical linear optimal control algorithm with displacement–velocity and velocity–acceleration feedbacks is used. The beam is composed by several linear springs with high stiffness as intermediate supports. A moving load and a moving mass were supposed to be the external excitations. The results signified the remarkable increase of the load inertial effects as the span number increased. However, it was revealed that the maximum response for beams with more spans occurs in larger values of the moving force velocity. Mahieddine *et al*. (2010) presented a partially delaminated piezoelectric beam to investigate its behavior using Euler-Bernoulli beam theory; the computed frequencies with the model based on the formulation presented in their work are in good agreement with the exact results. This shows the validity of the assumptions adopted in their work.

In this paper we take into account a piezoelectric bimorph beam made of a PVDF material, and we study its dynamic behavior considering a delamination zone between the upper and the lower layers. Its mathematical model has been established by the use of the FOSDT, the structural damping, the geometric configuration and the load nature. The numerical model developed will be compared with those of the literature to be validated.

2. Theoretical study

Let us consider a Timoshenko beam with the first order shear deformation theory (FOSDT), which gives the strains as a function of displacement of the neutral plane of the beam in Eq. (1). And neglecting the thermal effect, we can write the piezoelectric constitutive equations Eq. (2), (Liu *et al*. 2012, Zheng *et al*. 2002, Hai *et al*. 2009)

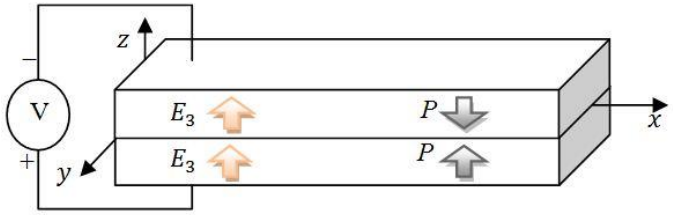

Fig. 1 Series configuration

$$\begin{cases} \varepsilon_x = u_{,x} - z\psi_{,x} \\ \gamma_{xz} = w_{,x} - \psi \end{cases} \tag{1}$$

and

$$\begin{cases} \sigma_{ij} = Q_{ijkl}\,\varepsilon_{kl} - e_{ijk}\,E_k \\ D_i = e_{ikl}\,\varepsilon_{kl} + \bar{\varepsilon}_{ik}\,E_k \end{cases} \tag{2}$$

Where ε_x, γ_{xz} are strains, u is axial displacement, ψ is the rotation and w is the vertical displacement of the neutral plane.

We note throughout this article that, the superscript t indicates the transpose of matrix, and the superscripts *T*, *B* indicate respectively the top and the bottom layer, the subscripts $X_{,x}$ and $X_{,z}$ denotes the x and z derivation. Introducing Voigt's notation the equations Eq. (2) become

$$\begin{cases} \sigma_p = Q_{pq}\,\varepsilon_q - e_{pk}\,E_k \\ D_i = e_{iq}\,\varepsilon_q + \bar{\varepsilon}_{ik}\,E_k \end{cases} \tag{3}$$

With σ, Q, e, E, D and $\bar{\varepsilon}$ are respectively stress, elastic coefficients, piezoelectric coefficients, electric field, dielectric displacement and permittivity (see Fig. 1 for the coordinate system). In matrix form we can write

$$\begin{cases} \{\sigma\} = [Q]\{\varepsilon\} - [e]^t\{E\} \\ \{D\} = [e]\{\varepsilon\} + [\bar{\varepsilon}]\{E\} \end{cases} \tag{4}$$

Taking into account the hypotheses related to the beam theory, namely:

- The stress vector is $\{\sigma\} = \{\sigma_x \quad \tau_{xz}\}^t$
- The strain vector is $\{\varepsilon\} = \{\varepsilon_x \quad \gamma_{xz}\}^t$
- $[Q], [\bar{\varepsilon}]$ and $[e]$ For PVDF materials.
- $\{E\} = \{0 \quad 0 \quad E_z\}$; $E_z = -\frac{\partial \phi}{\partial z} = \phi_{,z}$
- The electrical field has only one direction. ϕ is the electrode voltage.
- $\{D\} = \{0 \quad 0 \quad D_z\}$ Dielectric displacement of beam.
- The bimorph is in the anti-parallel or series configuration: as it is presented in Poizat and Benjeddou 2006, Smits *et al*. 1991 and Zemirline *et al*. 2013. (see Fig. 1).

P is the polarization direction of each layer. So, using these assumptions with Eq. (4) we obtained the results mentioned below Mahieddine (2011).

$$[Q] = \begin{bmatrix} Q_{11} & Q_{12} & Q_{13} & 0 & 0 & Q_{16} \\ Q_{21} & Q_{22} & Q_{23} & 0 & 0 & Q_{26} \\ Q_{31} & Q_{32} & Q_{33} & 0 & 0 & Q_{36} \\ 0 & 0 & 0 & Q_{44} & Q_{45} & 0 \\ 0 & 0 & 0 & Q_{54} & Q_{55} & 0 \\ Q_{61} & Q_{62} & Q_{63} & 0 & 0 & Q_{66} \end{bmatrix}; [e] = \begin{bmatrix} 0 & 0 & e_{31} \\ 0 & 0 & e_{32} \\ 0 & 0 & e_{33} \\ 0 & e_{24} & 0 \\ e_{15} & 0 & 0 \\ 0 & 0 & 0 \end{bmatrix}$$

$$\begin{cases} \sigma_x = \left(Q_{11} - \dfrac{Q_{12}^2}{Q_{22}}\right)\varepsilon_x - \left(e_{31} - \dfrac{Q_{21}}{Q_{22}}e_{32}\right)E_z \\ \tau_{xz} = \left(Q_{55} - \dfrac{Q_{45}^2}{Q_{44}}\right)\gamma_{xz} \end{cases}$$

$$\begin{Bmatrix} D_x \\ D_y \\ D_z \end{Bmatrix} = \begin{bmatrix} 0 & 0 & 0 & 0 & e_{15} & 0 \\ 0 & 0 & 0 & e_{25} & 0 & 0 \\ e_{31} & e_{32} & e_{33} & 0 & 0 & 0 \end{bmatrix} \begin{Bmatrix} \varepsilon_x \\ \varepsilon_y \\ \varepsilon_z \\ \gamma_{yz} \\ \gamma_{xz} \\ \gamma_{xy} \end{Bmatrix} + \begin{bmatrix} \bar{\varepsilon}_{11} & \bar{\varepsilon}_{12} & \bar{\varepsilon}_{13} \\ \bar{\varepsilon}_{21} & \bar{\varepsilon}_{22} & \bar{\varepsilon}_{23} \\ \bar{\varepsilon}_{31} & \bar{\varepsilon}_{32} & \bar{\varepsilon}_{33} \end{bmatrix} \begin{Bmatrix} E_x \\ E_y \\ E_z \end{Bmatrix}$$

$$D_z = \left(\bar{\varepsilon}_{33} + \frac{e_{32}^2}{Q_{22}}\right)E_z + \left(e_{31} - e_{32}\frac{Q_{21}}{Q_{22}}\right)\varepsilon_x$$

So we admit that

$$\bar{Q}_{11} = \left(Q_{11} - \tfrac{Q_{12}^2}{Q_{22}}\right) ;\ \tilde{e}_{31} = \left(e_{31} - \tfrac{Q_{21}}{Q_{22}}e_{32}\right) ;\ \bar{Q}_{55} = \left(Q_{55} - \tfrac{Q_{45}^2}{Q_{44}}\right) ;\ \bar{\bar{\varepsilon}}_{33} = \left(\bar{\varepsilon}_{33} + \tfrac{e_{32}^2}{Q_{22}}\right)$$

The deformation energy is given by

$$U = \frac{1}{2}\int_V (\varepsilon\sigma - DE)dV = \frac{1}{2}\int_V \left((\varepsilon_x\sigma_x + \gamma_{xz}\tau_{xz}) - D_zE_z\right)dV = U_{Elas} + U_{Piezo} + U_{Diélec} \tag{5}$$

Let h_{pT}, h_{pB} , b, L and V denote respectively the thicknesses of the top and bottom layers, the width, the length and the volume of the beam, we can found the following energies

$$U_{Elas} = \frac{1}{2}\int \{u\}^t[B]^t[H][B]\{u\}dx \tag{6}$$

$$\begin{aligned} U_{Piezo} = \frac{1}{2}b\int \Bigg(& \int_{-h_{pB}}^{0} [\phi_{,z}^{B}(u_{,x} + z\psi_{,x})\tilde{e}_{31}^{B} + (u_{,x} + z\psi_{,x})\tilde{e}_{31}^{B}\phi_{,z}^{B}]dz \\ & - \int_{0}^{h_{pT}} [\phi_{,z}^{T}(u_{,x} + z\psi_{,x})\tilde{e}_{31}^{T} + (u_{,x} + z\psi_{,x})\tilde{e}_{31}^{T}\phi_{,z}^{T}]dz \Bigg)dx \end{aligned} \tag{7}$$

$$U_{Diele} = -\frac{1}{2}b\int \left(\int_{-h_{pB}}^{0} \phi_{,z}^{B}\,\bar{\bar{\varepsilon}}_{33}^{B}\phi_{,z}^{B}\,dz + \int_{0}^{h_{pT}} \phi_{,z}^{T}\,\bar{\bar{\varepsilon}}_{33}^{T}\phi_{,z}^{T}\,dz\right)dx \tag{8}$$

The kinetic energy is given by

$$T = \frac{1}{2}\int \rho(\dot{u}^2 + \dot{v}^2 + \dot{w}^2)\,dV$$

$$T = \frac{b}{2}\int_0^L \left(\int_{-h_{pT}}^{0} \rho_{bot}\{\dot{u} \quad \dot{w} \quad \dot{\psi}\}[\bar{\bar{T}}]\begin{Bmatrix}\dot{u}\\ \dot{w}\\ \dot{\psi}\end{Bmatrix}dz + \int_0^{h_{pT}} \rho_{top}\{\dot{u} \quad \dot{w} \quad \dot{\psi}\}[\bar{\bar{T}}]\begin{Bmatrix}\dot{u}\\ \dot{w}\\ \dot{\psi}\end{Bmatrix}dz\right)dx \tag{9}$$

Where ρ, ρ_{top}, and ρ_{bot} are respectively the density of the whole beam, the density of the top layer and the density of the bottom layer. And $[\bar{\bar{T}}] = \begin{bmatrix} 1 & 0 & z \\ & 1 & 0 \\ Sym & & z^2 \end{bmatrix}$

After completing the calculations we have found the final form of the kinetic energy

$$T = \frac{b}{2}\int_0^L \{\dot{u} \quad \dot{w} \quad \dot{\psi}\}[\bar{T}]\begin{Bmatrix}\dot{u}\\ \dot{w}\\ \dot{\psi}\end{Bmatrix} dx \tag{10}$$

3. Finite element formulation

We take into consideration the beam shown in Fig. 3 which is composed of three zones. Two of them have two layers perfectly bonded and the other zone with two debonded layers. The structural and electric degrees of freedom are denoted in terms of the general degrees of freedom $\{q\}$, of each zone in the following manner.

3.1 1st and 3rd zones. The layers are perfectly bonded

$$\{u \quad w \quad \psi\}^t = N_b\{q\} \;;\; \{u_i \quad u_j\}^t = [N_{u\_b}]\{q\} \;;$$
$$\{w_i \quad w_j\}^t = [N_{w\_b}]\{q\} \;;\; \{\psi_i \quad \psi_j\}^t = [N_{\psi\_b}]\{q\}$$

with

N_{u_b}, N_{w_b} *and* N_{ψ_b} are a linear shape functions in the bonded zone.

3.2 2nd zone. The layers are debonded (*delaminated*)

$$\{u^T \quad u^B \quad w \quad \psi\}^t = N_d\{q\} \;;\; \{u_i^T \quad u_j^T\}^t = [N_{u_d}^T]\{q\} \;;\; \{u_i^B \quad u_j^B\}^t = [N_{u_d}^B]\{q\}$$
$$\{w_i \quad w_j\}^t = [N_{w\_d}]\{q\} \;;\; \{\psi_i \quad \psi_j\}^t = [N_{\psi\_d}]\{q\}$$

with

N_{u_d}, N_{w_d} *and* N_{ψ_d} are a linear shape functions in the debonded zone (See Mahieddine 2011, for more details).

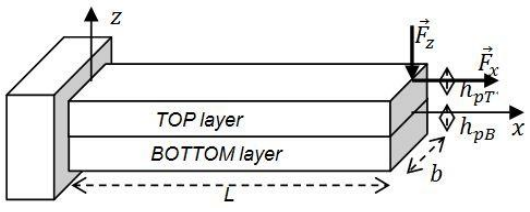

Fig. 2 Bimorph dimensions

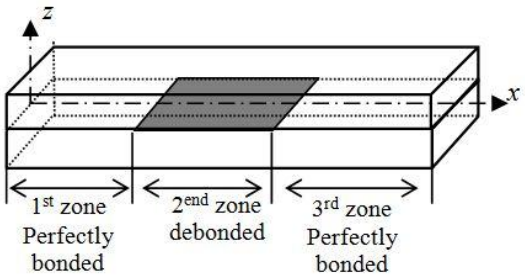

Fig. 3 Localization of delamination zone

$$\phi^B = \left[N_\phi^B\right]\{\phi_1 \quad \phi_2 \quad \phi_3\}^t \quad ; \quad \phi^T = \left[N_\phi^T\right]\{\phi_1 \quad \phi_2 \quad \phi_3\}^t$$

ϕ^B and ϕ^T are top and bottom voltages. ϕ_i ; $i = 1, 2, 3$ Are the electrodes voltages (in the top, middle and bottom faces).

We obtain the following elementary matrices:

In the bonded zone (1st and 3rd zones)

$$U_{Elas} = \frac{1}{2}\{q\}^t [K_{uu-b}]^e \{q\} \tag{11}$$

$$U_{Piezo} = \frac{1}{2}\{q\}^t \left[K_{u\phi\_b}\right]^e \{\phi\} + \frac{1}{2}\{\phi\}^t \left[K_{\phi u\_b}\right]^e \{q\} \tag{12}$$

$$U_{Diele} = \frac{1}{2}\{\phi\}^t \left[K_{\phi\phi}\right]\{\phi\} \tag{13}$$

$$T = \frac{bl^e}{4}\{\dot{q}\}^t [M_b]\{\dot{q}\} \tag{14}$$

$[K_{uu-b}]^e \equiv$ [6 X 6] Matrix size, $\left[K_{u\phi\_b}\right]^e \equiv$ [6 X 3] Matrix size, $\left[K_{\phi u\_b}\right]^e \equiv$ [3 X 6] Matrix size.

In the debonded zone (2nd zone)

$$U_{Elas} = \frac{1}{2}\{q\}^t [K_{uu-d}]^e \{q\} \tag{15}$$

$$U_{Piezo} = \frac{1}{2}\{q\}^t \left[K_{u\phi\_d}\right]^e \{\phi\} + \frac{1}{2}\{\phi\}^t \left[K_{\phi u\_d}\right]^e \{q\} \tag{16}$$

U_{Diele} : still the same

$$T = \frac{bl^e}{4}\{\dot{q}\}^t [M_d]\{\dot{q}\} \tag{17}$$

$[K_{uu-d}]^e \equiv$ [8 X 8] Matrix size, $\left[K_{u\phi\_d}\right]^e \equiv$ [8 X 3] Matrix size, $\left[K_{\phi u\_d}\right]^e \equiv$ [3 X 8] Matrix size.

4. Equation of motion

When assembling all the obtained elementary matrices taking into account the Hamilton principle we obtain the equation of motion which is written in the following matrix form Xiangjian *et al*. 2012, and Hai *et al*. 2009.

$$[M]\{\ddot{\bar{q}}\} + [C]\{\dot{\bar{q}}\} + [K]\{\bar{q}\} = \{F\} \tag{18}$$

$$[M] = \begin{bmatrix}[M_{uu}] & [0] \\ [0] & [0]\end{bmatrix} \; ; \quad [K] = \begin{bmatrix}[K_{uu}] & \left[K_{u\phi}\right] \\ \left[K_{\phi u}\right] & \left[K_{\phi\phi}\right]\end{bmatrix} ; \quad [C] = \begin{bmatrix}[C_{uu}] & [0] \\ [0] & [0]\end{bmatrix} \; ; \quad \{\bar{q}\} = \begin{Bmatrix}\{q\} \\ \{\phi\}\end{Bmatrix}$$

$[C_{uu}] = \alpha[M_{uu}] + \beta[K_{uu}]$

$[M_{uu}]$: Is the global mass matrix. $[K_{uu}]$: Is the global stiffness matrix.

$[C_{uu}]$: Is the global damping matrix. $\{F\}$: Is the external load vector.

α & β : Are the Rayleigh coefficients, which describe the damping attitude of the structure.

5. Results and discussions

To solve the obtained equations of motion for the bimorph, we consider the Newmark method and we use the Matlab code. After the confrontation of the results obtained for a bimorph made of two piezo-layers with those obtained by Perel and Palazotto 2002, we obtain Table 1, which shows the results compared with two configurations. The first one, the two layers have the same thickness. In the second one, the two layers have 0.007 m in the bottom layer and 0.003 m in the top layer. Taking into account the following PVDF properties, and the geometric dimensions of the clamped-free beam.

$$E_1 = E_2 = 2\text{e}9\ \text{N/m}^2;\ G_{12} = 7.75\text{e}8\ \text{N/m}^2;\ \nu = 0.29\ ;\ d_{31} = 2.2\text{e}-11\ \text{C/N}\ ;$$

$$\bar{\bar{\varepsilon}}_{11} = \bar{\bar{\varepsilon}}_{22} = \bar{\bar{\varepsilon}}_{33} = 1.62\text{e}-11\ \text{F/m}$$

$$L = 0.4\ \text{m},\qquad b = 0.05\ \text{m}\ \text{ and }\begin{cases} h_{pT} = h_{pB} = 0.005\ \text{m}. \\ h_{pT} = 0.003\ \&\ h_{pB} = 0.007\ \text{m}. \end{cases}$$

We present the following tables of comparisons. In case of a perfectly bonded clamped-free beam Table 1. In case of delaminated clamped-free beam Table 2. The errors seen in Table 1 indicate that our results are close to the analytical ones of Perel and Palazotto 2002, which don't take in consideration the shear deformation effect, for the low frequencies.

Table 2 presents the frequencies of several beams which have a delamination zone (DZ) with several lengths and positions, we observe that the natural frequency of the beam decreases if the beam presents a delamination zone (DZ). The natural frequencies computed of several beams with

Table 1 Comparison between the present work and Perel and Palazotto 2002: The 8 first frequencies of two beams, the first beam made of two equal layers, and the second with different layer thicknesses

	Frequency (Hz)	Analytical Perel	Perfectly Bonded	Error		Analytical Perel	Perfectly Bonded	Error
hTop = hBot = 0.005 (m)	1st Freq	10.641	10.641	0.00%	*hTop* = 0.003 & *hBot* = 0.007 (m)	10.641	10.668	-0.25%
	2nd Freq	66.749	66.639	0.16%		66.749	66.657	0.14%
	3rd Freq	186.711	186.380	0.18%		186.711	185.767	0.51%
	4th Freq	365.914	364.629	0.35%		365.914	361.581	1.18%
	5th Freq	604.927	601.474	0.57%		604.927	592.609	2.04%
	6th Freq	903.702	658.809	27.10%		903.702	658.809	27.10%
	7thFreq	1262.117	896.158	29.00%		1262.117	876.174	30.58%
	8th Freq	1680.400	1247.811	25.74%		1680.400	1209.281	28.04%

Table 2 Presentation of the 8 first frequencies of two delaminated beams, the first beam made of two equal layers, and the second with different layer thicknessesd

	Frequency (Hz)	Lengths of bimorph (Bonded zone ; Debonded zone ; Bonded zone)						
		L/6;L/3;L/2	L/3;L/3;L/3	L/2;L/3;L/6	L/4;L/2;L/4	L/3;L/3;L/3	5L/12;L/6;5L/12	5L/6;L/12;5L/6
hTop = hBot = 0.005 (m)	1st Freq	10.335	10.405	10.507	9.879	10.405	10.631	10.659
	2nd Freq	58.185	65.794	63.457	62.229	65.794	66.600	66.624
	3rd Freq	172.031	137.199	168.490	116.868	137.199	173.317	184.128
	4th Freq	269.253	307.962	254.186	241.801	307.962	358.560	361.341
	5th Freq	461.311	455.455	451.332	419.408	455.455	505.061	576.929
	6th Freq	658.809	658.809	658.809	636.862	658.809	658.809	658.808
	7thFreq	675.767	660.865	672.209	658.809	660.865	836.792	874.605
	8th Freq	945.928	944.828	943.638	819.045	944.828	1017.649	1147.988
hTop = 0.003 & *hBot* = 0.007 (m)	1st Freq	10.473	10.515	10.574	10.195	10.515	10.646	10.660
	2nd Freq	61.299	66.140	64.759	64.010	66.140	66.598	66.599
	3rd Freq	177.707	152.595	175.857	133.599	152.595	178.292	184.620
	4th Freq	293.056	328.833	281.947	274.799	328.833	359.243	360.737
	5th Freq	500.645	484.929	493.396	467.751	484.929	535.405	581.848
	6th Freq	658.699	658.682	658.745	658.377	658.682	659.020	659.131
	7thFreq	723.963	716.773	721.295	696.510	716.773	851.598	872.018
	8th Freq	1023.617	1023.368	1023.022	902.976	1023.368	1065.752	1168.141

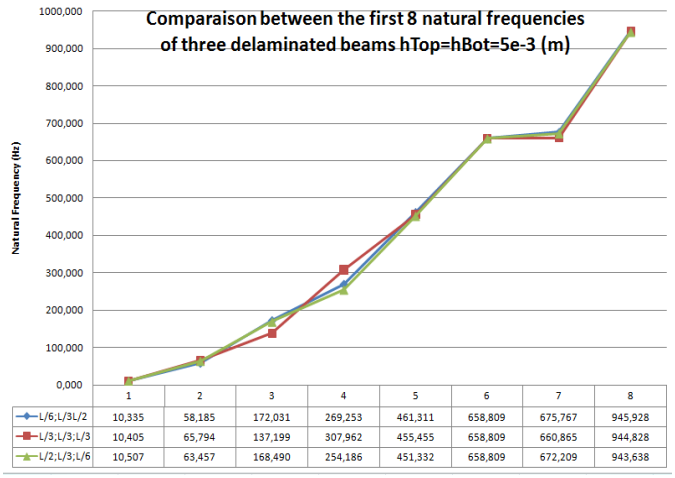

Fig. 4 The first 8th natural frequencies of three beams with different DZ lengths, hTOP = hBOT

different (DZ) positions are equal when the (DZ) position is symmetric to the middle of the beam's length. See Figs. 4-5.

As a result of the confrontation between the present work and those of the literature we can admit that the results of the present work are in good agreement with those of literature.

Now we consider the same beam with the following two configurations of boundary conditions, a clamped-free and a clamped-clamped configuration. We apply a uniformly distributed load on the beam, with considering two thicknesses, the first $h_{Top} = h_{Bot} = 5e-3$ m, and the second $h_{Top} = 3e-3$; $h_{Bot} = 7e-3$ m. The axial displacement is given by the following figures.

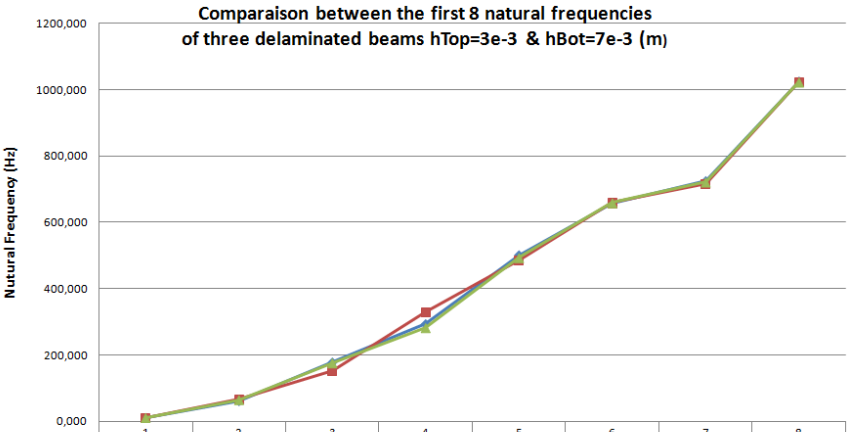

	1	2	3	4	5	6	7	8
L/6;L/3;L/2	10,473	61,299	177,707	293,056	500,645	658,699	723,963	1023,617
L/3;L/3;L/3	10,515	66,140	152,595	328,833	484,929	658,682	716,773	1023,368
L/2;L/3;L/6	10,574	64,759	175,857	281,947	493,396	658,745	721,295	1023,022

Fig. 5 The first 8th natural frequencies of three beams with different DZ lengths, hTOP ≠ hBOT

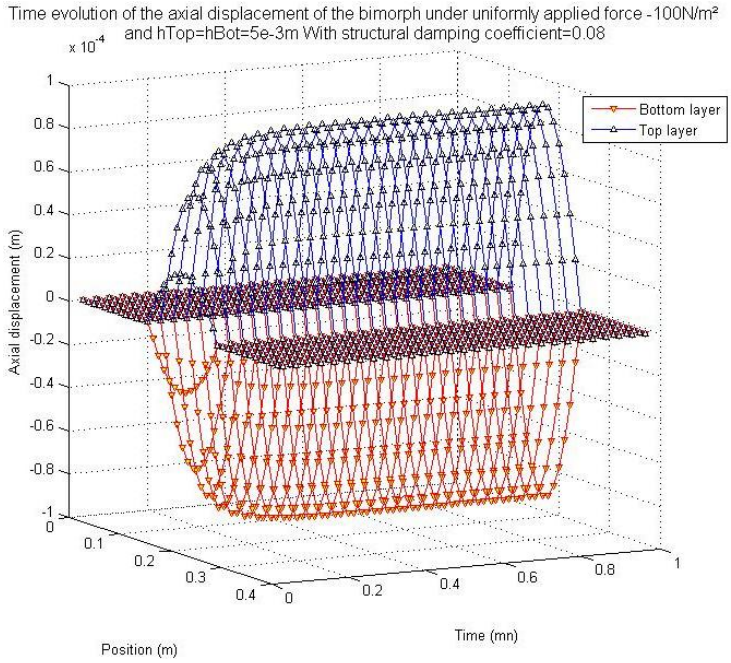

Fig. 6 Axial displacement evolution under uniformly applied charge *hTOP = hBOT* on a simply supported beam

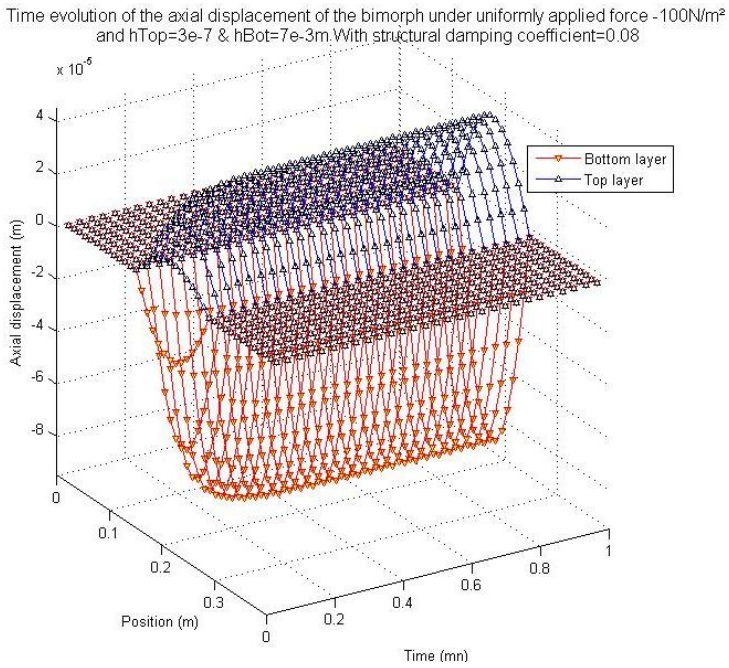

Fig. 7 Axial displacement evolution under uniformly applied charge *hTOP* ≠ *hBOT* on a simply supported beam

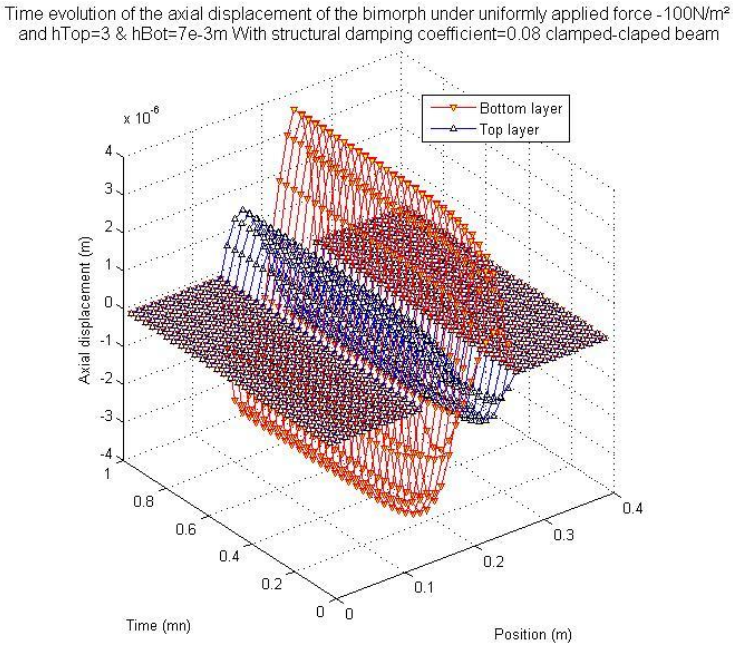

Fig. 8 Axial displacement evolution under uniformly applied charge *hTOP* ≠ *hBOT* on a clamped-clamped beam

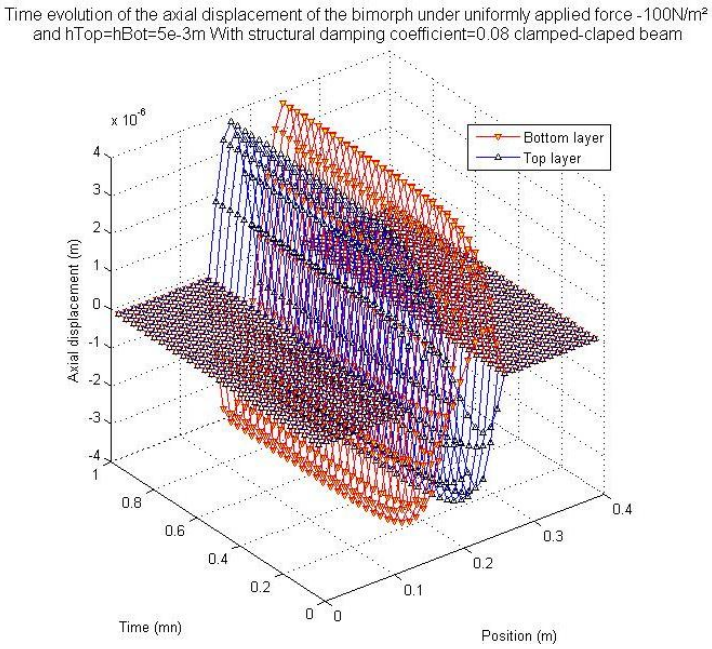

Fig. 9 Axial displacement evolution under uniformly applied charge *hTOP = hBOT* on a clamped-clamped beam

However, the vertical displacement is given by

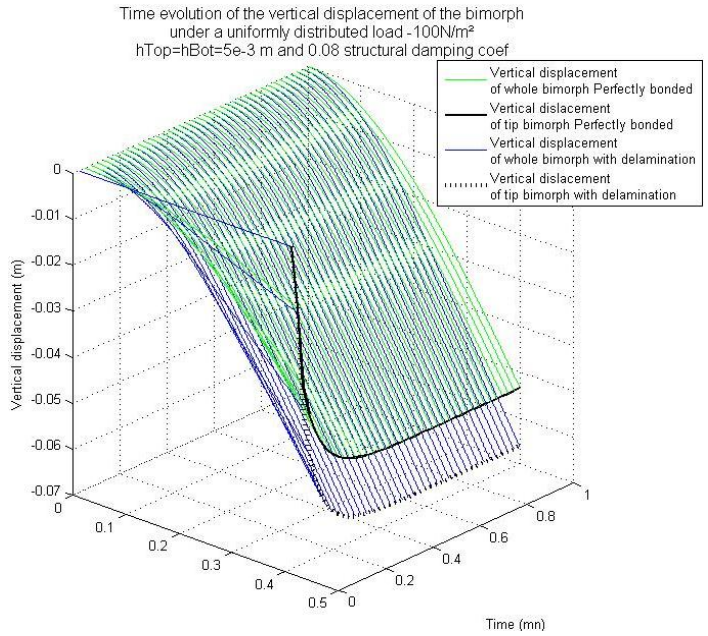

Fig. 10 The evolution of the vertical displacement of two beams (perfectly bonded and debonded) *hTOP = hBOT*

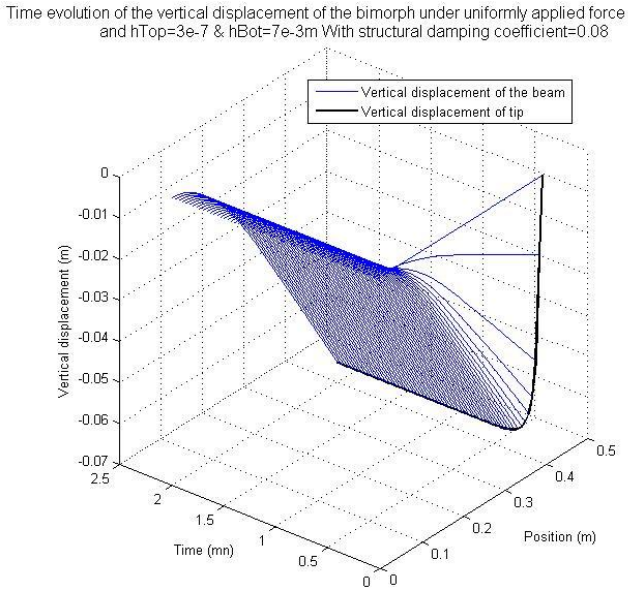

Fig. 11 The evolution of the vertical displacement of a perfectly bonded beam *hTOP ≠ hBOT*

In Figs. 6, 7, 8 and 9, the evolution of the axial displacement is treated. We can observe that the thickness of the upper and the lower layer affects the axial displacement. A field of an axial displacement related to the delamination zone appears. This field rises when the thickness of the layer increases. Besides, the boundary conditions affect this field when the beam is clamped in its both sides. Positive and negative values can be seen with the same magnitudes in this displacement field.

In Figs. 10 and 11, when the beam presents a debonded zone, the vertical displacement is affected too, it seems clearly that the rise of the vertical displacement is due to the delamination zone, the thickness changes of the top (or bottom layer) don't affect the vertical displacement, as long as the thickness of the whole beam stay the same.

In the harmonic case, which means the applied charge is a voltage applied on the top and the bottom electrodes, called V^{Top} and V^{Bot} that have a harmonic form like: $V^{Top} = Vcos(8t)$.

$V^{Bot} = Vcos(8t + \varphi)$; φ is the dephasing (or the phase angle) between the upper and lower voltages. Similar to the work of Arafa *et al 2009*. Who applied a trapezoidal signal with a $\frac{\pi}{2}$ phase angle on the upper and lower layers.

In Fig. 12, 13 and 14, a beam with delamination zone produces more actuation in its tip than a perfectly bonded beam. The effect of the structural damping coefficient is felt, a beam with a higher structural damping coefficient produces less actuation than a beam with lower coefficient. The same observation in Figs. 10 and 11 related to the distribution of thicknesses between the two layers is noted.

Figs. 15, 16, 17, 18 and 19 symmetric trajectories are produced relatively to the thickness distribution, (if the thickness ratio is inverted between the upper and lower layer, the produced trajectory shape is reversed). The delamination affects the trajectory shape, and increases the actuation in the vertical direction. The length of the beam doesn't affect the shape, it only affects the values of the trajectory, and the same observation is noticed about the structural damping

coefficient. The dephasing changes (or the phase angle changes) between the upper and lower applied voltages give new trajectories. So, we can change the dephasing value to obtain specific actuations.

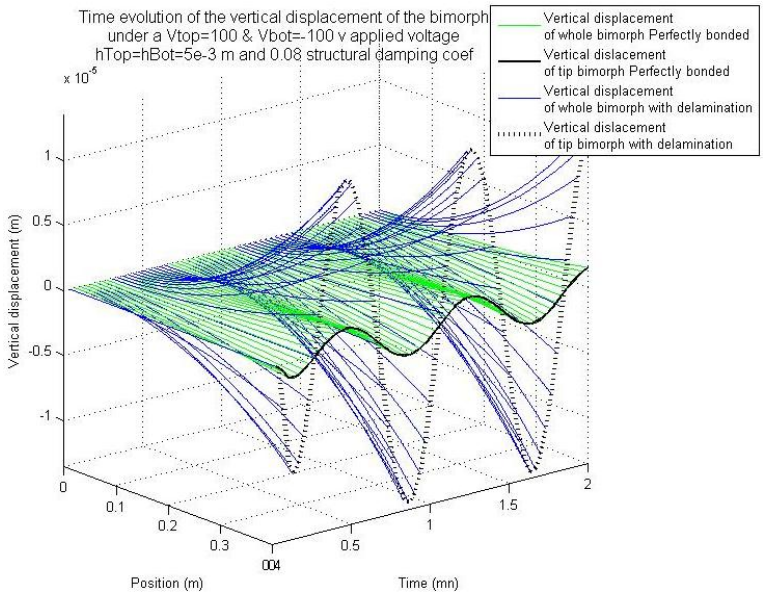

Fig. 12 The vertical displacement under an applied electric voltage for two beams (perfectly bonded and debonded)

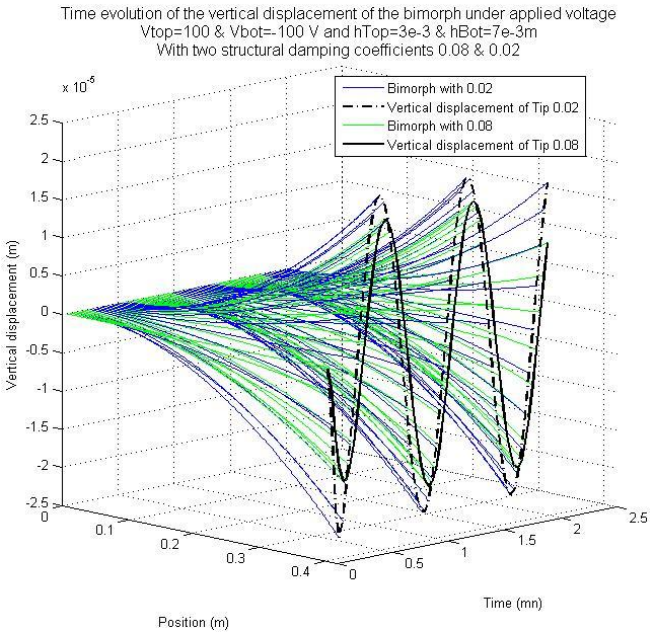

Fig. 13 The vertical displacement under an applied electric voltage for two beams with different structural damping coefficient *hTOP* ≠ *hBOT*

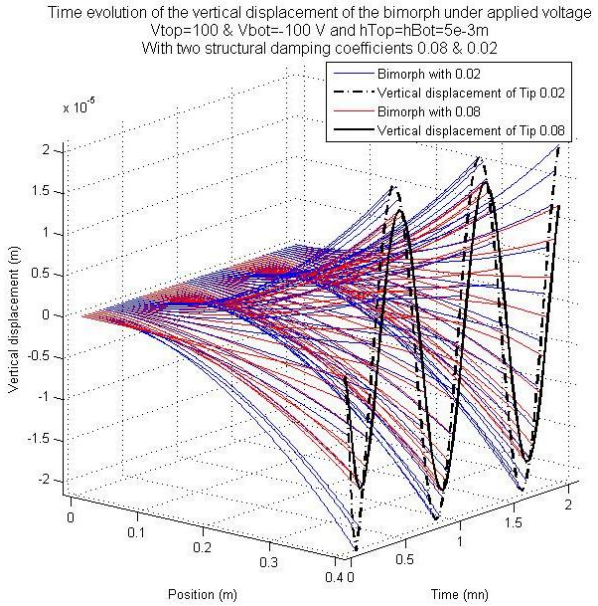

Fig. 14 The vertical displacement under an applied electric voltage for two beams with different structural damping coefficient *hTOP = hBOT*

The effect of the delamination on the trajectory of the tip beam is treated below.

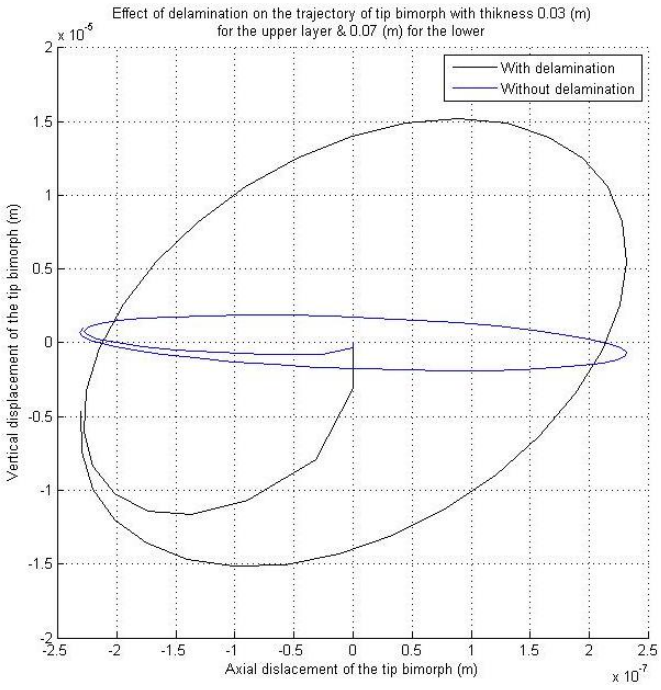

Fig. 15 The trajectory of tip beam changes under the effect delamination *hTOP* = 0,03 & *hBOT* = 0,07 m

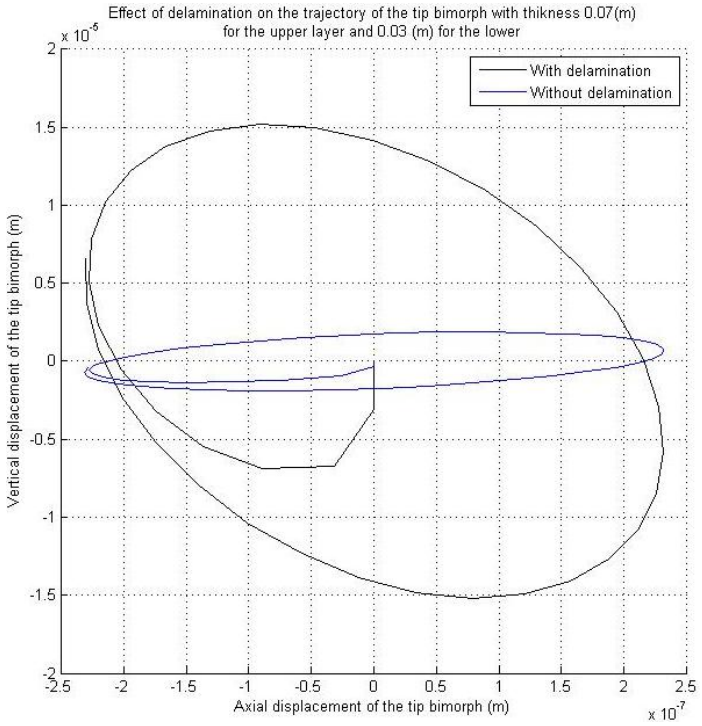

Fig. 16 The trajectory of tip beam changes under the effect delamination *hTOP* = 0,07 & *hBOT* = 0,03 m

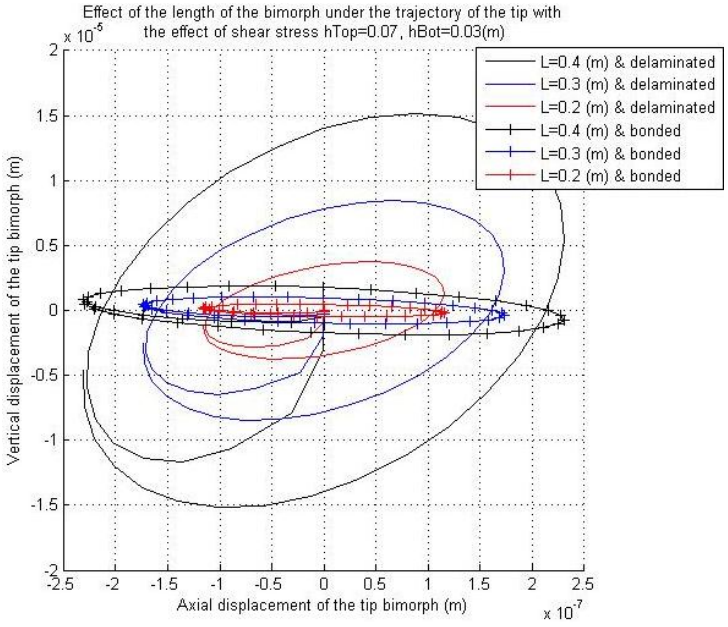

Fig. 17 The effect of shear stress on the trajectory of the tip beam

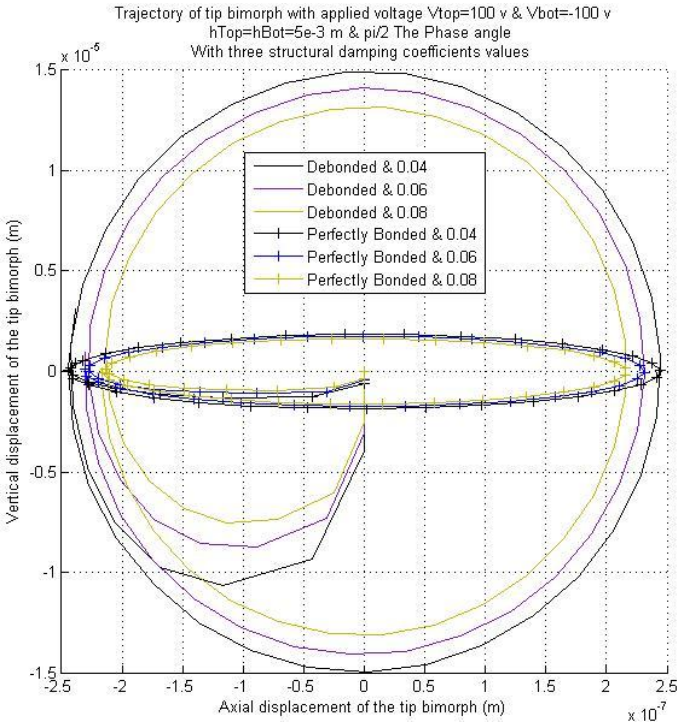

Fig. 18 The effect of phase angel on the trajectory of the tip beam

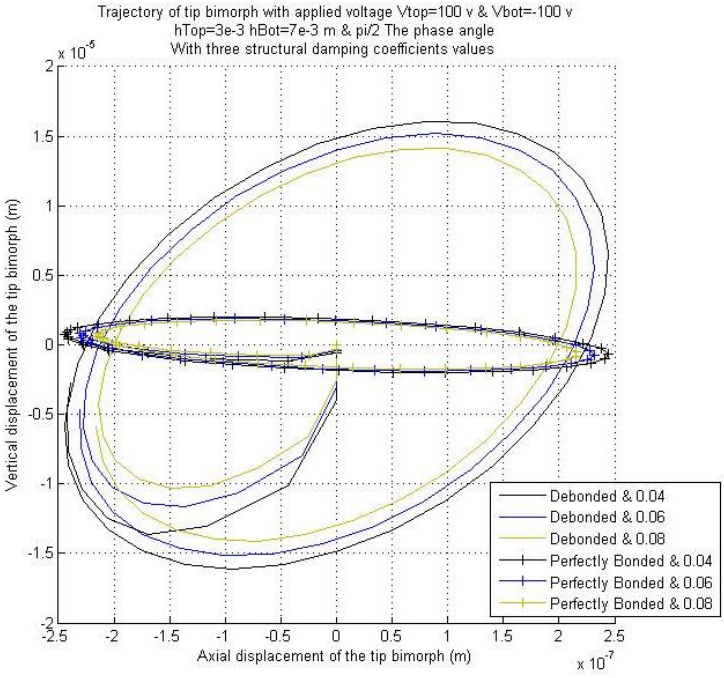

Fig. 19 The effect of the structural damping coefficient on the trajectory of the tip beam

6. Conclusions

We have studied the dynamic behavior of a bimorph beam made of two piezoelectric layers. The effect of delamination zone between the upper and the lower layer is presented with taking into account the effect of: the shear deformation (the FOSDT), the thickness variation, the size, the location of the delamination zone, the structural damping, the nature of the load (stationary or harmonic) and the phase angle (between the upper and the lower layer). A finite element method was used for modeling the problem. We have chosen the NEWMARK method to solve the set of equations for the beam motion. For this purpose, the Matlab software is used to carry out the full calculations. In order to validate our model, the results are confronted with those of literature. Results show that the boundary conditions and the thickness of the piezoelectric layers affect the axial displacement field related to the delamination zone. The vertical displacement is affected by the delamination zone, and the actuation in the free tip increases. The structural damping and the length of the beam affect only the values (without affecting the shape) of the trajectory of the free end of the beam.

Acknowledgments

The authors would like to acknowledge Mr. A. Abdellah El Hadj professor from the LMP2M (Laboratoire de Mécanique Physique et Modélisation Mathématique. Ain d'Dheb, University of Medea, Algeria), for his support and helpful advice. And Mr Meghraoui Nadjib for his assistance.

References

Arafa, M., Aldraihem, O. and Baz, A. (2009), "Modeling and characterization of a linear piezomotor", *J. Intell. Mater. Syst. Struct.*, 2**0**(16), 1-9. DOI: 10.1177/1045389X09343022

Donoso, A. and Sigmund, O. (2009), "Optimization of piezoelectric bimorph actuators with active damping for static and dynamic loads", *Struct. Multidisc. Optim.*, **38**(2), 171-183.

Hai, A., Weiguang, A., Duohe, Y. and Binsheng, W. (2009), "Static force reliability analysis of truss structure with piezoelectric patches affixed to its surface", *Chinese J. Aeronaut.*, **22**(1), 22-31.

Li, Y.S., Feng, W.J. and Cai, Z.Y. (2014), "Bending and free vibration of functionally graded piezoelectric beam based on modified strain gradient theory", *Compos. Struct.*, **115**, 41-50.

Lui, X., Chen, R. and Zhu, L. (2012), "Energy conversion efficiency of rainbow shape piezoelectric transducer", *Chinese J. Aeronaut.*, **25**(5), 691-697.

Mahieddine, A. (2011), "Effets de la piézoélectricité et de l'amortissement structural dans le cas des poutres, des coques et des plaques. Contrôle actif", Ph.D. Dissertation; Saad Dahleb University of Blida, Algeria.

Mahieddine, A., Pouget, J. and Ouali, M. (2010), "Modeling and analysis of delaminated beams with integrated piezoelectric actuators", *Comptes Rendus Mécanique*, **338**(5), 283-289.

Nikkhoo, A. (2014), "Investigating the behavior of smart thin beams with piezoelectric actuators under dynamic loads", *Mech. Syst. Signal Process.*, **45**(2), 513-530.

Perel, V.Y. and Palazotto, A.N. (2002), "Finite element formulation for dynamics of delaminated composite beams with piezoelectric actuators", *Int. J. Solid. Struct.*, **39**(17), 4457-4483.

Poizat, C. and Benjeddou, A. (2006), "On analytical and finite element modelling of piezoelectric extension and shear bimorphs", *Comput. Struct.*, **84**(22-23), 1426-1437.

Smits, J.G., Dlake, I. and Cooney, T.K. (1991), "The constituent equations of piezoelectric bimorphs", *Sens. Actuat. A*, **28**(1), 41-61.

Zemirline, A., Ouali, M. and Mahieddine, A. (2013), "Actuation using piezoelectric bimorph beams under the effects of structural damping", *Proceeding of the Contech Conference*, Istanbul, Turkey, December.

Zheng, X.J., Zhou, Y.C. and Nin, M.Z. (2002), "Thermopiezoelectric response of a piezoelectric thin film PZT-6B deposited on MgO(1 0 0) substrate due to a continuous laser", *Int. J. Solid. Struct.*, **39**(15), 3935-3957.

Zhou, Y-G., Chen, Y-M. and Ding, H-J. (2007), "Analytical modeling of sandwich beam for piezoelectric bender elements", *Appl. Math. Mech.*, **28**(2), 1581-1586.

CC